

A hyaena on stilts: Comparison of the limb morphology of *Ictitherium ebu* (Mammalia: Hyaenidae) from the Late Miocene of Lothagam, Turkana Basin, Kenya with extant Canidae and Hyaenidae (#92989)

1

First submission

Guidance from your Editor

Please submit by **8 Jan 2024** for the benefit of the authors (and your token reward) .



Structure and Criteria

Please read the 'Structure and Criteria' page for general guidance.



Author notes

Have you read the author notes on the [guidance page](#)?



Raw data check

Review the raw data.



Image check

Check that figures and images have not been inappropriately manipulated.

If this article is published your review will be made public. You can choose whether to sign your review. If uploading a PDF please remove any identifiable information (if you want to remain anonymous).

Files

Download and review all files from the [materials page](#).

17 Figure file(s)
20 Table file(s)
1 Raw data file(s)
1 Other file(s)




Structure and Criteria

Structure your review

The review form is divided into 5 sections. Please consider these when composing your review:

1. BASIC REPORTING
2. EXPERIMENTAL DESIGN
3. VALIDITY OF THE FINDINGS
4. General comments
5. Confidential notes to the editor






 You can also annotate this PDF and upload it as part of your review

When ready [submit online](#).





Editorial Criteria

Use these criteria points to structure your review. The full detailed editorial criteria is on your [guidance page](#).




BASIC REPORTING

-  Clear, unambiguous, professional English language used throughout.
-  Intro & background to show context. Literature well referenced & relevant.
-  Structure conforms to [PeerJ standards](#), discipline norm, or improved for clarity.
-  Figures are relevant, high quality, well labelled & described.
-  Raw data supplied (see [PeerJ policy](#)).

EXPERIMENTAL DESIGN

-  Original primary research within [Scope of the journal](#).
-  Research question well defined, relevant & meaningful. It is stated how the research fills an identified knowledge gap.
-  Rigorous investigation performed to a high technical & ethical standard.
-  Methods described with sufficient detail & information to replicate.

VALIDITY OF THE FINDINGS

-  Impact and novelty not assessed. *Meaningful* replication encouraged where rationale & benefit to literature is clearly stated.
-  All underlying data have been provided; they are robust, statistically sound, & controlled.
-  Conclusions are well stated, linked to original research question & limited to supporting results.



The best reviewers use these techniques

Tip

Example

Support criticisms with evidence from the text or from other sources

Smith et al (J of Methodology, 2005, V3, pp 123) have shown that the analysis you use in Lines 241-250 is not the most appropriate for this situation. Please explain why you used this method.

Give specific suggestions on how to improve the manuscript

Your introduction needs more detail. I suggest that you improve the description at lines 57- 86 to provide more justification for your study (specifically, you should expand upon the knowledge gap being filled).

Comment on language and grammar issues

The English language should be improved to ensure that an international audience can clearly understand your text. Some examples where the language could be improved include lines 23, 77, 121, 128 – the current phrasing makes comprehension difficult. I suggest you have a colleague who is proficient in English and familiar with the subject matter review your manuscript, or contact a professional editing service.

Organize by importance of the issues, and number your points

1. Your most important issue
2. The next most important item
3. ...
4. The least important points

Please provide constructive criticism, and avoid personal opinions

I thank you for providing the raw data, however your supplemental files need more descriptive metadata identifiers to be useful to future readers. Although your results are compelling, the data analysis should be improved in the following ways: AA, BB, CC

Comment on strengths (as well as weaknesses) of the manuscript

I commend the authors for their extensive data set, compiled over many years of detailed fieldwork. In addition, the manuscript is clearly written in professional, unambiguous language. If there is a weakness, it is in the statistical analysis (as I have noted above) which should be improved upon before Acceptance.

A hyaena on stilts: Comparison of the limb morphology of *Ictitherium ebu* (Mammalia: Hyaenidae) from the Late Miocene of Lothagam, Turkana Basin, Kenya with extant Canidae and Hyaenidae

Julien van der Hoek^{Corresp., 1}, Lars Werdelin²

¹ Department of Earth and Environmental Sciences, University of Manchester, Manchester, Greater Manchester, United Kingdom

² Department of Palaeobiology, Swedish Museum of Natural History, Stockholm, Stockholm County, Sweden

Corresponding Author: Julien van der Hoek
Email address: julien.vanderhoek@manchester.ac.uk

The long, gracile morphology of the limb bones of the Late Miocene hyaenid *Ictitherium ebu* has led to the hypothesis that this animal was cursorial. The forelimb and femur of the holotype were compared with specimens of extant Hyaenidae and Canidae. Two morphometric methods were used. The first used measurements to calculate indices of different morphological characters. The second method involved capturing photographs of the anterior distal humerus of each specimen, mapping six landmarks on them, and calculating truss distances. These distances represent a schematic reproduction of the elbow. Multivariate statistical analysis primarily separated the data based on taxonomy, yet locomotor and habitat categories were also considered. *Ictitherium ebu* has an overall morphology similar to that of the maned wolf and a distal humerus reminiscent of that of the aardwolf. The long, gracile limb bones of *I. ebu* are suggested to be adaptations for pouncing on prey, for locomotor efficiency, and for looking over the tall grass of the open environments the animal lived in, much like the present-day maned wolf.

1 A hyaena on stilts: Comparison of the limb morphology of
2 Ictitherium ebu (Mammalia: Hyaenidae) from the Late
3 Miocene of Lothagam, Turkana Basin, Kenya with extant
4 Canidae and Hyaenidae

5
 6 J. van der Hoek¹, L. Werdelin²

7 ¹Department of Earth and Environmental Sciences, University of Manchester, Manchester,
 8 Greater Manchester, United Kingdom.

9 ²Department of Palaeobiology, Swedish Museum of Natural History, Stockholm, Stockholm
 10 County, Sweden

11
 12 Corresponding Author:
 13 Julien van der Hoek¹

14
 15 Dover Street, Manchester, Greater Manchester, M13 9NT, United Kingdom

16 Email address: julien.vanderhoek@postgrad.manchester.ac.uk

Abstract

The long, gracile morphology of the limb bones of the Late Miocene hyaenid *Ictitherium ebu* has led to the hypothesis that this animal was cursorial. The forelimb and femur of the holotype were compared with specimens of extant Hyaenidae and Canidae. Two morphometric methods were used. The first used measurements to calculate indices of different morphological characters. The second method involved capturing photographs of the anterior distal humerus of each specimen, mapping six landmarks on them, and calculating truss distances. These distances represent a schematic reproduction of the elbow. Multivariate statistical analysis primarily separated the data based on taxonomy, yet locomotor and habitat categories were also considered. *Ictitherium ebu* has an overall morphology similar to that of the maned wolf and a distal humerus reminiscent of that of the aardwolf. The long, gracile limb bones of *I. ebu* are suggested to be adaptations for pouncing on prey, for locomotor efficiency, and for looking over the tall grass of the open environments the animal lived in, much like the present-day maned wolf.

Introduction

Hyaenidae is a family of considerable palaeontological interest, due to their occurrence in many Miocene-Pleistocene sites in Eurasia (Kurtén, 1968; Turner, Antón & Werdelin, 2008) and the significance of the three larger species of hyaenids for their respective ecosystems (Rieger, 1981; Mills, 1982; Turner, Antón & Werdelin, 2008; Hayssen & Noonan, 2021). The pattern of their evolution in Eurasia is clear. They started off as viverrid- and herpestid-like forms, which, through canid-like and cursorial forms, over time evolved into the bone crushing animals we know today (Turner, Antón & Werdelin, 2008). During the Miocene-Pliocene mammalian turnover the number of cursorial, canid-like hyaenid species decreased, while the number of Canidae increased. Few bone-crushing hyaenids are known from the latest Miocene, whereas they show up more prominently during the Pliocene. During the Pleistocene Hyaenidae became increasingly adapted to bone-crushing, with the more cursorial morphotypes disappearing.

This clear pattern is contrasted with community patterns in Late Miocene Africa, which are not yet well understood, especially when compared to the evolutionary pattern of Eurasia (Werdelin, 2003). The carnivore material from Lothagam (Kenya) may allow for such an investigation to take place (Werdelin, 2003), in part through better understanding of the ecological roles of the species found in this material.

Lothagam is a Miocene-Pliocene site located near Lake Turkana in Turkana County, Kenya (Fig. 1). It has been dated from 8 to slightly less than 4 Ma (Leakey, 2003). The exceptional preservation of fossils at the site is due to the initial accumulation of sediment from a large meandering river system. Massive faulting led to the formation of a horst, which has kept the fossils from being buried. The resistance of the fine-grained matrix of most of the site has also contributed to the preservation. It is an important site for mammal palaeontology, as it is the type site for seven genera and 21 species of mammal. The carnivoran fauna of Lothagam includes Amphicyonidae, Mustelidae, Viverridae, Hyaenidae, Felidae and Canidae and resembles Langebaanweg in South Africa in overall structure (Werdelin,

2003). The hyaenid fauna of Lothagam includes *Ictitherium ebu*, *Hyaenictitherium cf. H. parvum*,
cf. Hyaenictis sp., and *Ikelohyaena cf. I. abronia*. The first two species have been identified as
jackal/wolf- like ecomorphotypes, *Hyaenictis* as a genus of cursorial meat eaters, and *I. abronia*
as a transitional bone cracker (Coca-Ortega & Pérez-Claros, 2019).

The holotype of *I. ebu*, KNM-LT 23145, was found in the Lower Nawata Member of the Nawata
Formation (Werdelin, 2003). This formation represents fluvial facies that show fluctuations in
water **budget** and subsidence rate (Feibel, 2003). The Lower Nawata Member is characterised by
conglomerate beds of varying thickness, sandstones, and mudstones, together with volcanic
detritus with a large amount of intercalated altered distal tephra. The age of the Lower Nawata is
 7.4 ± 0.1 to 6.5 ± 0.1 Ma (McDougall & Feibel, 2003). The palaeosols of the Lower Nawata
mainly represent relatively open grassland, gallery woodland and thornbush savanna (Wynn,
2003). Pure grassland has not been recorded in the palaeosols, meaning that it was likely not
long-lived if present. The Lower Nawata is characterised by the presence of Bovidae,
Hippopotamidae, Suidae and Cercopithecidae, which indicate a well-vegetated habitat (Leakey &
Harris, 2003).

Of the four hyaenids found at Lothagam, *I. ebu* is by far the best preserved, as it includes both
postcranial and craniodental material (Werdelin, 2003). It has dentition that is seemingly adapted
for a more hypercarnivorous lifestyle than other members of *Ictitherium*. This lifestyle seems to
be supported by the notably long slender limbs of the species, which could be interpreted as an
adaptation for cursoriality. The ecology and behaviour of canid-like hyaenids has been mentioned
as needing further investigation (Turner, Antón & Werdelin, 2008). The present study provides
insight into the ecology of a canid-like hyaenid, as well as the apparent cursorial adaptations of *I.*
ebu.

Extant carnivorans can be classified into different locomotor categories, such as arboreal,
scansorial, terrestrial and semi-fossorial, as shown by **Van Valkenburgh (1987)**. By comparing
body mass and skeletal measurements using bivariate and multivariate analysis, it was found that
skeletal indicators can predict locomotor behaviour in extant carnivorans. This technique was
also applied to extinct carnivorans, with partial success. Van Valkenburgh (1987) noted that the
characters that define locomotor behaviour in extant carnivorans might differ from those of
extinct carnivorans. However, if the biomechanical function of each part of an extinct carnivoran
is understood, then it should be possible to reconstruct its locomotor behaviour as well.

Samuels, Meachen and Sakai (2013) and Andersson (2004) expanded upon the methods of Van
Valkenburgh (1987). Samuels, Meachen and Sakai (2013) expanded on the skeletal indicators
and added cursorial and semi-aquatic categories. Andersson (2004) applied truss analysis (Strauss
& Bookstein, 1982) to the distal humerus to separate grappling from non-grappling predators.
These two methods are here combined to test the hypothesis that *I. ebu* was adapted for
cursoriality.

Determining the ecomorphology of *I. ebu* will not only shed light on the ecological role of this species but can ultimately contribute to a better understanding of the ecology of the Late Miocene communities of Lothagam and eastern Africa as a whole. Furthermore, the comparisons might reveal whether *I. ebu* had an ecomorphology that converges on the Canidae, among which many species are cursorially adapted (Samuels, Meachen & Sakai, 2013). *Ictitherium* was part of the jackal and wolf-like meat eater ecomorph of Werdelin and Solounias (1996) (see also Turner, Antón & Werdelin, 2008; Coca-Ortega & Pérez-Claros, 2019). This ecomorphology would then be in line with hyaenids in Eurasia having a more cursorial, canid-like morphology before being replaced by canids (Werdelin & Turner, 1996; Turner, Antón & Werdelin, 2008).

The objectives of this study are (1) to create models capable of predicting the ecomorphology of *I. ebu*. (2) to test the hypothesis that *I. ebu* was cursorial. (3) to gain a broader understanding of the ecomorphology of *I. ebu*.

Materials & Methods

To be able to test if *I. ebu* was adapted for cursoriality, the appendicular skeleton of different extant carnivorans, of which the ecomorphology is known, were compared to the holotype of *I. ebu*, KNM-LT 23145 from the Nawata Formation. The method of Samuels, Meachen & Sakai (2013) was adapted to study the appendicular skeleton as a whole, while the method of Andersson (2004) was used to study the distal humerus. Due to these two different sets of methods utilising two different datasets, the results and discussion sections will be presented separately for the two datasets.

Because *I. ebu* is hypothesized to be a cursorial hyaenid, with cursorial adaptations similar to those of Canidae (Coca-Ortega & Pérez-Claros, 2019), only canids and hyaenids were selected. The four extant Hyaenidae were included in the study as they represent the closest living relatives to *I. ebu*. While the spotted hyaena (*Crocuta crocuta*), the striped hyaena (*Hyaena hyaena*), and the brown hyaena (*Parahyaena brunnea*) are cursors, the aardwolf (*Proteles cristatus*) has a more generalist locomotor type (Mills, 1982; Spoor & Badoux, 1988; Koehler & Richardson, 1990; Hayssen & Noonan, 2021). The Canidae in this study include a wide range of sizes from the small red fox (*Vulpes vulpes*) to the medium sized coyote (*Canis latrans*) and side-striped jackal (*Lupulella adusta*) and the large wolf (*Canis lupus*). The maned wolf (*Chrysocyon brachyurus*) was primarily included for its morphology, as its long, slender limbs bear a resemblance to those of *I. ebu*.

Specimen collection

The remains used for the study of *Ictitherium ebu* include the manus, radius, ulna, humerus and femur of a cast of specimen KNM-LT 23145 from the Late Miocene of Lothagam, Kenya, housed in the National Museums of Kenya (NMK) (Fig. 2). A tibia is present as well, but it is broken at the diaphysis, which limits its relevance to this study. The collections of Naturhistoriska Riksmuseet (NRM), Museum für Naturkunde (ZMB), Senckenberg Naturmuseum (SMF), Alexander Koenig Zoological Research Museum (ZFMK), Royal Museum

for Central Africa (RMCA), Naturalis Biodiversity Center (RMNH) and La Specola (MZUF) were visited to collect photographs and measurements of 79 specimens of extant species for comparison with KNM-LT 23145 (Table 1). Adult specimens of both sexes were chosen, with a preference for wild-caught individuals.

Linear morphometrics

Specimens were measured according to the measurement protocol of Samuels *et al.* (Samuels & Van Valkenburgh, 2008; Samuels, Meachen & Sakai, 2013), with an added measurement for the midshaft mediolateral diameter of the radius (RD) (Fig. 3, Table 2). The measurement for FGT was carried out differently from the one of Samuels *et al.* (Samuels & Van Valkenburgh, 2008; Samuels, Meachen & Sakai, 2013), where the height of the greater trochanter of the femur was measured vertically instead of diagonally.

The measurements were taken with vernier callipers for measurements up to 15 cm. Measuring tape was used for measurements above 15 cm in all museums except for the Museum für Naturkunde in Berlin, where the measurements were carried out with larger callipers. Measurements were recorded to the nearest 0.1 cm (Table S1).

Index calculations

The measurements were then converted into indices (Samuels & Van Valkenburgh, 2008; Samuels, Meachen & Sakai, 2013) in Excel 16.0.15330.20260 (Table 3, Dataset S1). The manus proportions index was excluded from further analysis due to a lack of measurements. The radial robustness index, metacarpal radial index, humeral femoral index and metacarpal humeral index were included to be able to take into account the metacarpal III measurements and the relationship between the humerus and the femur.

For initial interpretation, preliminary boxplots of the indices plotted against species were created. These boxplots revealed some outliers in the measurements, among which some are measurement errors. These values were often far too extreme to be viewed as simple extremes in the data. For example, the humeral epicondylar breadth of ZMB MAM 82516 was measured to be half that of the other specimens, while the length is within the range of the other specimens. With the use of ImageJ 1.53n to approximate what measurement would have been obtained on-site, it was determined that 10 outliers needed to be removed from the dataset (Table S2). Aside from these outliers, there were some missing values in the dataset. For these missing values, means were interpolated in MS Excel 16.0.15330.20260 for species with missing indices by using the mean of the same index for the other specimens of the same species. Boxplots were recreated for the final analysis, with all of these changes incorporated.

Truss analysis

The distal humerus of each specimen was photographed in anterior view. The camera was set to have an ISO of 200/250, an aperture of F8-F10, after which the shutter speed was adjusted for brightness. Photographing was carried out with flash. The scale bar was held in place using two

alligator clips on 4-way swivels, at the height of the specimen. Some photographs appeared overexposed after data collection. These images were edited using GIMP 2.10.30 with lowering of highlights and lowering the point at which highlights turn to white. The specimens edited in this manner were SMF 97379, SMF 97380 and ZMB MAM 89495. For a test of the validity of the photographs and removal of invalid photographs, see Article S1, Dataset S1, Table S3, Table S4 and Fig. S1.

Truss creation

Using TpsUtil64 1.81 a TPS file was created from the photographs acquired during data collection. The TPS file was imported into TpsDig264 2.32, labelled and scaled according to the scalebar in each image. Six landmarks were assigned to each specimen following Andersson (2004) (Fig. 4). The coordinates of the landmarks for each specimen were exported to Excel 16.0.15330.20260 using MorphoJ 1.07a (Table S4), after which the distances of the truss were calculated (Dataset S1).

Statistics

All tests were carried out in RStudio 2022.12.0 (Posit team, 2023) and R version 4.2.2 (R Core Team, 2022). The code and complementary files can be found in Dataset S1. Both the linear morphometric and the Truss dataset were found to be largely non-parametric by using a Shapiro-Wilks normality test (Shapiro & Wilk, 1965) on every index and distance (Table S5, Table S6). Boxplots were created of the 13 indices of the linear morphometrics. Colours for plots were selected using the webpage “Coloring for colorblindness” (Nichols, 2023). Plots were created using ggplot2, ggtext, ggpubr and tidyverse packages (Wickham, 2016; Wickham et al., 2019; Wilke & Wiernik, 2022; Kassambara, 2023). Silhouettes of the different extant species were acquired through PhyloPic (Keesey, 2023).

Permutational multivariate analysis of variance

Permutational multivariate analysis of variance (PERMANOVA) (Anderson, 2001) was used for analysis of the linear morphometrics. It tests if the centroids of a group of objects are the same. The test is a non-parametric alternative to multiple analysis of variance (MANOVA). The assumption for PERMANOVA is that the observations are exchangeable under the null hypothesis. Therefore, objects must be independent and have similar multivariate dispersion.

Assumption tests for similar multivariate dispersion were carried out using the vegan package (Oksanen et al., 2022). A multivariate analogue of Levene's test for homogeneity of variances (betadisper) (Anderson, 2006) was used with Euclidean distances, after which an analysis of variance (ANOVA) (Fisher, 1921), as well as a permutation test of multivariate homogeneity of group dispersions (permutest) (Legendre, Oksanen & ter Braak, 2011) were used to validate the assumption of similar multivariate dispersion.

For species, the ANOVA yielded a p of 0.002, while the permutest yielded a p of 0.011, both of which are significant ($\alpha = 0.05$). For family both results were significant as well, with the

ANOVA and permutest yielding a p of 0.004 and 0.005 respectively. Thus, multivariate dispersion was not similar, which can cause the test to be too conservative when there is large dispersion in groups of large numbers of samples and too liberal when there is large dispersion in groups of small numbers of samples (Anderson & Walsh, 2013). **See the discussion for limitations of the statistics.**

A two-way PERMANOVA with Euclidean distances and 999 permutations was carried out to compare the indices between family and species, using the function `adonis2` from the `vegan` package (Oksanen et al., 2022). Species is nested in family, therefore the performed PERMANOVA is nested as well. Post-hoc Holm-corrected pairwise PERMANOVAs were carried out to identify differences **in variance** between pairs of species using the function `pairwise.adonis` from the wrapper function `PairwiseAdonis` (Holm, 1979; Martinez Arbizu, 2020). The Holm method of post-hoc correction is a more powerful sequentially rejective Bonferroni correction.

Non-metric multidimensional scaling

Non-metric multidimensional scaling (NMDS) (Kruskal, 1964) with a maximum of 999 random restarts, two dimensions and Euclidean distances was carried out using the function `metaMDS` from the `vegan` package (Oksanen et al., 2022) for both the indices as well as the Truss distances. Its goal is to plot dissimilar objects far apart from each other and similar objects close together in ordination space (Legendre & Legendre, 1998). First, a distance matrix is constructed using Euclidean distances, as the data are non-ecological. A number of dimensions is chosen, in our case $k=2$ for ease of interpretability. An initial configuration is chosen; in the case of `metaMDS`, this is done with metric scaling (Oksanen et al., 2022). This initial configuration is important, as the solution to the algorithm that is used depends partly on this configuration (Legendre & Legendre, 1998).

A matrix of fitted distances is calculated, then compared to the initial distances using monotone regression (which is non-metric) fitted by least-squares (Legendre & Legendre, 1998). Goodness of fit (stress) is used to evaluate the regression, which measures how far the new configuration is from being monotonic to the original distances. It is a relative measure, as it only measures the decrease in lack-of-fit between iterations in this procedure. The configuration is then moved slightly in the direction in which stress decreases the most rapidly (Kruskal, 1964; Legendre & Legendre, 1998). The matrix is then recalculated, and steps are repeated until a minimum lack-of-fit is reached and no more progress can be made or until a tolerated lack-of-fit is reached (Legendre & Legendre, 1998). These then become the coordinates of our two-dimensional ordination. In our case, the programme is allowed to carry out up to 999 random restarts before the process is halted (Oksanen et al., 2022). Data are then centred, as well as rotated so that the first principal component will be on the first axis. The variable scores of the NMDS were used to explain the ordination. The NMDS results were validated using a Shepard diagram and goodness of fit of individual points (Dexter, Rollwagen-Bollens & Bollens, 2018), using the `stressplot` and goodness functions of the `vegan` package (Oksanen et al., 2022). These are available in the supplementary material (Fig. S2, Fig. S3, Table S7, Table S8).

Stepwise flexible discriminant analysis

Stepwise variable selection was carried out for species, family, locomotion and habitat on both datasets. Using a greedy Wilk's lambda F-test (Mardia, Kent & Bibby, 1979) from the klaR package (Weihs et al., 2005) the indices were selected based on an F-test decision of 0.05 (Table S9-Table S12). The variable selection works by defining a start variable that separates the group most, then selects additional variables (Weihs et al., 2005). It makes this selection based on the Wilk's lambda criterion, which means it selects the one which minimises Wilk's lambda of the model, adding more variables if the p-value still shows statistical significance ($p = 0.05$). The data were divided into 30% training data and 70% validation data using the caret and tidyverse packages (Wickham et al., 2019; Kuhn, 2022). The training data were then used to carry out flexible discriminant analysis (FDA) (Hastie, Tibshirani & Buja, 1994) for each variable using the function fda from the mda package (Hastie et al., 2022). Flexible discriminant analysis works as an adaptation of linear discriminant analysis (LDA) (Hastie, Tibshirani & Buja, 1994). Linear discriminant analysis finds a reduced number of discriminate coordinate functions to be able to optimally separate groups. This number is always the number of groups minus one. The non-parametric multiresponse regression technique BRUTO (Hastie, 1989) was used for FDA. It generates a very large base set automatically, then achieves parsimony by shrinking coefficients in a sensible, structured manner (Hastie, Tibshirani & Buja, 1994). The function "bruto" in the mda package functions by fitting a model by adaptive backfitting using smoothing splines (Hastie et al., 2022). The number of adaptive models is equal to the number of response variables in the model, but for each variable the same amount of smoothing is used. The variable can either be omitted, linear, or fitted by a smoothing spline. During each step of the backfitting procedure, model selection is based on an approximation of the generalised cross-validation criterion (Hastie, Tibshirani & Buja, 1994; Hastie et al., 2022). Once selection has finished, the model is backfitted using the chosen amount of smoothing (Hastie et al., 2022). This model is then validated by testing how accurately the model predicts the validation data using the "predict" function from base-R (R Core Team, 2022). The variable most similar to *I. ebu* was predicted in each model using the same function.

Results

Linear morphometrics

Analysis of variance

A two-way permutational analysis of variance (PERMANOVA) was carried out on the indices to compare species and family (Table 4). Species were nested in family and 999 permutations were run. Both groupings are significant. The pseudo-F-statistic is much higher for family than for species, indicating more pronounced group separation between the two families than between individual species.

Pairwise one-way PERMANOVAs were carried out with post-hoc Holm corrections, revealing significant differences between some of the species (Table S13, Table S14). Boxplots of the 13

indices were generated to visually compare the different species (Fig. 5, Fig. S4, Fig. S5). The indices show the highest number of significant differences between the maned wolf and the other species (43 significant indices). Aside from *I. ebu*, the brown hyaena, and the coyote, which do not have enough specimens to have significant values for differences, the side striped jackal shows the lowest number of significant differences (17 significant indices). The indices HEI (24), FEI (22), and BI (22) provide the highest number of significant differences (Fig. 5), while URI (12), HFI (10), and HRI (6) provide the lowest number of significant differences.

Non-metric multidimensional scaling

A convergent solution was found after 20 tries by the model. Stress for the non-metric multidimensional scaling is 0.13. The Shepards plot shows an R^2 of the non-metric fit of 0.98 (Fig. S2). In the goodness of fit table (Table S7), none of the values of goodness of fit are above 0.05. There is a large amount of overlap in the data, particularly in the centre-left of the plot (Fig. 6).

Axis 1 of the NMDS is primarily controlled by SMI and HEI (Table 5). SMI represents the muscles acting across the shoulder joint while HEI represents the relative area for the origins of the forearm flexors, pronators, and supinators. Canids plot more on the left side and hyaenids more on the right side.

Axis 2 is primarily controlled by OLI, URI and RRI. OLI relates to the muscles used in elbow extension, while RRI is the indicator for radial robustness and stress resistance. URI represents the overall robustness and resistance to stress of the ulna. All these indices relate to the robustness of the forearm and extension of the elbow. The maned wolf, aardwolf and striped hyaena plot low on this axis, while the red fox, coyote and spotted hyaena plot high. While the aardwolf overlaps all Canidae except the red fox, the other Hyaenidae do not show overlap with the Canidae. The aardwolf and maned wolf, which are the two non-cursorial species, plot close together. *I. ebu* plots in the polygon formed by the maned wolf as well as the aardwolf.

Flexible discriminant analysis

Stepwise flexible discriminant analysis was performed on the 13 morphometric indices, of which 9 were selected using a greedy Wilk's lambda F-test. The indices FEI, BI, HFI, MCRI, HEI, GI, OLI, URI and MCHUM were selected based on an F-test decision of 0.05 (Table S9). The resulting plot of the first two axes has some overlap in the centre, with the coyote, wolf and aardwolf overlapping each other.

Together, the first two dimensions account for 69.96% of the data. The first dimension accounts for 46.72% of the data, while the second dimension accounts for 23.24% of the variance. The test data were predicted by the model with an accuracy of 0.8.

The red fox is separated from the rest of the data and clusters to the left (Fig. 7). The more cursorial Hyaenidae plot together on the right. In the centre are the other Canidae and the aardwolf, with the maned wolf plotted lower on CV2. When *I. ebu* is added to the model, it is predicted to be a maned wolf specimen.

Three other models were generated based on family, locomotion and habitat. As FDA reduces the dimensions of the tested groups by one, these were one-dimensional models (Fig. 8). The family model predicted the test data with an accuracy of 0.86. *I. ebu* scores a low value on CV1 and was predicted as Canidae, which is incorrect. The locomotion model predicted the test data with an accuracy of 0.77. *I. ebu* was predicted as cursorial and has an intermediate value on CV1. Finally, the habitat model predicted the test data with an accuracy of 1 and *I. ebu* was predicted as an open habitat species and has a value slightly above intermediate for the plot.

Truss analysis

Non-metric multidimensional scaling

A repeat of the best solution was reached after 26 tries. Stress is 0.03. The Shepards plot shows an R^2 of the non-metric fit of 0.99 (Fig. S3) and no goodness of fit value is higher than 0.01 for the individual points (Table S8). There is a lot of overlap between species, mainly on the left side of the plot (Fig. 9).

The first axis is mostly controlled by 5-6, the distal width of the trochlea, and 4-5, the distal width of the capitulum (Table 6). It reflects overall size. The second axis is primarily controlled by 5-6 and 2-5 and relates to the distal extension of the trochlea. It separates species like the wolf, with a less extended trochlea and squarer anterior distal humerus, from species like the striped hyaena, with a more extended trochlea. *I. ebu* is separated from the other species, indicating an intermediate size and trochlear extension.

Flexible discriminant analysis

The model accounts for 89.81 % of the variance in its first two dimensions. CV1 accounts for 52.46% of the variance. It reflects the shape of the capitulum and with it, the overall anterior distal humerus from a squarer (wolf) to a more rectangular (brown hyaena) shape. CV2 accounts for 37.35% of the variance. It reflects the overall size of the specimens (Fig. 10). Model accuracy is 0.72. It separates species in a manner similar to the NMDS. When *I. ebu* is added to the model, it is predicted as being a specimen of the aardwolf.

Three other models were generated based on family, locomotion and habitat. As FDA reduces dimensions of the tested groups by one, these were one-dimensional models (Fig. 11). The family model predicted the test data with an accuracy of 0.95. *I. ebu* was predicted as Hyaenidae and has a relatively high value on the plot. The locomotion model predicted the test data with an accuracy of 0.71. *I. ebu* had a high value and was predicted as having a generalist locomotor mode. Finally, the habitat model predicted the test data with an accuracy of 0.81 and *I. ebu* was predicted as an open habitat species with a relatively high value.

Discussion

Implications of the linear morphometrics

Variance

The permutational analysis of variance demonstrates that there are significant differences between the morphometric indices of families, as well as between species (Table 4). Indices HEI, FEI and BI have the most significant differences in the pairwise PERMANOVAs, showing that forelimb length and epicondylar breadth are important characteristics when separating species (Fig. 5, Table S13). These are also important characteristics for separating cursorial carnivores from other groups (Samuels, Meachen & Sakai, 2013), indicating that these indices detect similar differences in morphology in this smaller dataset.

While *Ictitherium ebu* has no significant pairwise comparisons due to only being a single individual, it can be visually separated from other species in the boxplots (Fig. 5, Fig. S4, Fig. S5). The animal has lower than average values of OLI, GI, RRI, HEI, FEI, HFI and a high BI. Except for GI and HFI, these indices are in the range of those of the maned wolf. The maned wolf and *I. ebu* also show overlap in SMI, OLI, URI, MCHUM and MCRI, meaning that they overlap in 10 of the 13 different indices, suggesting similar overall proportions and thus adaptations.

Non-metric multidimensional scaling

The first axis of the NMDS mainly discriminates between the two families. As SMI and HEI correlate quite well with these variables, it seems that relative deltopectoral crest size and epicondylar size have a phylogenetic signal. However, these differences are also due to size, as most hyaenids are larger than most canids.

Forearm robustness and the relative size of the olecranon are important explanatory variables for NMDS2. The maned wolf, aardwolf and striped hyaena all plot lower on NMDS2. They all have a shorter olecranon, which reflects the fact that these predators do not need to apply much strength with their forelimbs during hunting and handling prey (Martín-Serra, Figueirido & Palmqvist, 2016). Furthermore, they have less robust forearms. The striped hyaena is predominantly a scavenger (Rieger, 1981) and thus plots lower than the spotted hyaena, which more commonly hunts large prey (Hayssen & Noonan, 2021). The maned wolf and aardwolf are generalist species. *I. ebu* plots within the range of the maned wolf, not far from the aardwolf, indicating some overlap with these species in forearm function. Overall, it appears that NMDS2 reflects shape that is impacted by hunting strategy and cursoriality.

Flexible discriminant analysis

The flexible discriminant analyses predict *I. ebu* to be a maned wolf, Canidae, cursorial and open habitat. These findings contradict each other. In large part these contradictions exist due to the different indices used for the different models, making comparisons more difficult.

The species FDA somewhat resembles the NMDS, with *I. ebu* predicted as a maned wolf. This is not surprising, because in the NMDS *I. ebu* is plotted within the point cloud of the maned wolf and has quite similar morphology to this gracile-limbed animal. *I. ebu* is predicted as Canidae in the family model, indicating a more canid-like morphology. Of course, effects of size must be accounted for, but the animal is quite similar in overall morphology to the maned wolf, a canid. As a hyaenid from the Miocene, *I. ebu* also falls in a group of less robust, more canid-like, primitive hyaenids, which would be replaced by the more robust Hyaenidae of the post-Miocene (Coca-Ortega & Pérez-Claros, 2019).

A model with just three indices, OLI, MCRI and HFI, predicts *I. ebu* to be cursorial, which contradicts the NMDS, where *I. ebu* is plotted in the point clouds of the two generalist species. It also contradicts the similarity of *I. ebu* and the maned wolf. *I. ebu* plots in the area where the locomotor groups overlap, and there are more cursorial species in the dataset. Finally, *I. ebu* is predicted to be an open habitat species, which is in agreement with the NMDS and overall similarity to the maned wolf. The validation test here gives a value of 1, which is very high. This result is likely due to random chance, as both test and training datasets were acquired randomly.

Implications of the Truss analysis

Non-metric multidimensional scaling

The first axis of the NMDS reflects overall size, whereas NMDS2 reflects the extension of the trochlea. A size pattern was observed by Andersson (2004), where species <10kg are quite uniform in the main principal component that reflects shape. At 10-80 kg, the differences increase with size.

This pattern can be observed in the NMDS as well, even with the different loadings of NMDS1 and NMDS2. The smaller extant species (red fox, side-striped jackal, coyote and aardwolf) all plot around the 0-value of NMDS2. The larger extant Hyaenidae and Canidae are split into the low-scoring brown hyaena, striped hyaena and spotted hyaena and the higher scoring maned wolf and wolf. The Hyaenidae have lower values on NMDS2 due to more extended medial trochlear flanges. This extension reflects an increase in lateral stability during humeral articulation, which is an indicator of an animal that grapples with its prey (Andersson, 2004). Andersson (2004) placed both Hyaenidae and Canidae in a group with the cheetah (*Acinonyx jubatus*) to indicate non-grapplers. Only the maned wolf is interpreted as a grappler but has the elbow joint morphology of a non-grappler (Andersson, 2004). However, of note is that if figure 6 from Andersson (2004) is compared to the NMDS, the figures show the same difference between the larger canids and hyaenids.

Flexible discriminant analysis

I. ebu is predicted to be an aardwolf, Hyaenidae, generalist and open habitat by the different models of the discriminant function analysis. These models use the same truss distances and can

thus also be more easily compared with each other. None of the models contradict each other, as the **aardwolf is a generalist**, open habitat hyaenid. The NMDS would predict similar results, because *I. ebu* plots closest to the aardwolf in the NMDS. The species model even resembles the NMDS, although shape is more important than size. Furthermore, *I. ebu* does not plot in areas of overlap in any of the one-dimensional analyses.

Implications of the combined morphometric methods

Size explains a large amount of dissimilarity in all of the species plots. However, on the first axis of the linear morphometrics results family seems to be the main distinguishing factor. For the species FDA of the truss analysis, size even appears to be secondary to shape, as the main axis of variance represents the shape of the capitulum.

The presence of a phylogenetic signal within the shape variables cannot be eliminated because extant canids have a cursorial ancestry (Andersson, 2004). This can be seen in the maned wolf, a generalist species that has traits of a more cursorial animal (Andersson, 2004; Samuels, Meachen & Sakai, 2013).

A pattern emerges when the morphometric methods are analysed together. While a quick look at the variance showed a closer similarity of *I. ebu* to the maned wolf in the **overall morphology of the limb bones, both the maned wolf and aardwolf showed similar values in the NMDS**. The species FDA predicted *I. ebu* to be similar to the maned wolf, far from the other species data. The truss analysis of the distal humerus showed a closer affinity to the aardwolf in both the NMDS and species FDA.

While family was predicted as Canidae in the linear analysis, the truss analysis interpreted the family as Hyaenidae. It may be that the morphology of *I. ebu* is overall more similar to Canidae, but the elbow is more similar to Hyaenidae. While the locomotor model predicts cursorial locomotion for the overall morphology, the elbow predicts generalist locomotion. However, both species predictions would suggest a generalist animal. The models interpret *I. ebu* as an open habitat animal, in agreement with Werdelin (2003). The Lower Nawata represents a relatively mixed habitat, as pure grassland was likely not long-lived but could have been present (Wynn, 2003). Therefore, *I. ebu* could have been present during a short time when there were pure grasslands. Other explanations for the presence of an open-habitat species in mixed habitat are that species do not always live in their ideal habitat, or that the animal was drawn to the location to drink and died there.

Overall, the long, gracile limbs of *I. ebu* were not an adaptation for cursoriality, but for being able to look over the tall grasses of its environment and pounce on prey, similar to the maned wolf (Hildebrand, 1954; Janis & Wilhelm, 1993) and possibly the serval (*Leptailurus serval*), a felid not analysed here that removes prey from crevices (Janis & Wilhelm, 1993; Ewer, 1998). The longer legs of *I. ebu* also contribute to its walking efficiency, as locomotion efficiency increases with longer legs at all gaits (Pennycuick, 1975; Janis & Wilhelm, 1993).

Limitations of the research

Data collection

Only three of the nine spotted hyaena specimens used in this study had completely fused epiphyses (ZMB MAM 7784, ZMB MAM 13295 and ZMB MAM 47515), which is normally the main indicator of an adult animal. However, according to Egeland, Egeland & Bunn (2008), sub-adulthood is characterised by unfused or partially fused epiphyses with solid bone surfaces. Sponginess only occurs at near-epiphyses. Adults have epiphyses that are mostly or completely fused, with the entire surface of the bone being solid. Specimens ZMB MAM 14818, ZMB MAM 16575, and ZMB MAM 82415 have fused epiphyses with entirely solid bone surfaces; only thin grooves show the epiphyses to not be entirely fused. They could thus be interpreted as adult specimens. ZMB MAM 82413, ZMB MAM 82471 and ZMB MAM 82516 do not have fused epiphyses, but do not show much spongy bone around the epiphyses. These specimens can then be interpreted as older sub-adults. The striped hyaena ZMB MAM 82363 also had a humerus that was not fully fused, which would indicate a subadult if interpreted in the same way as the spotted hyaena specimens (Egeland, Egeland & Bunn, 2008). However, it does not have any measurements that are below the range of the other specimens. Only the radial diameter is smaller than the others, but three specimens have equally small radial diameters. Truss distances all fall within the range of other specimens. MZUF 13354 (wolf) illustrates the difference between zoo animals and wild animals quite accurately. In the species dataset, MZUF 13354 has the most extreme value for every single index, with 8 outliers. The short bones of this animal are the likely cause of these values.

Statistics

Sample sizes differed for the species, with the brown hyaena and coyote having merely represented by two and one specimens, respectively. The permutational analysis of variance could have been affected as a consequence of this unbalanced design. While PERMANOVA can handle unbalanced designs, it can be affected by heterogeneous dispersions (Anderson & Walsh, 2013; Anderson et al., 2017). Use of the betadisper test for homogeneity of variances, followed by ANOVA and permutest found heterogeneous dispersions in the data. The NMDS shows a pattern that clearly separates species by size and morphology. The pairwise PERMANOVAs serve to identify significant differences between species more specifically.

Conclusions

Ictitherium ebu was hypothesised to be cursorial, based on its long, gracile limbs. Through a combination of two and three dimensional morphometric techniques it was found that *I. ebu* resembled the maned wolf in the overall morphology of the limbs, while it resembled the aardwolf in the morphology of the knee joint. As neither of these animals is cursorial, *I. ebu* would not have been cursorial either. Similar to the maned wolf, the long slender limbs of *I. ebu* would have been an adaptation for looking over the tall grasses of its environment, pouncing on prey and walking efficiency. Further research on the ecomorphology of the hyaenids of Lothagam and other Late Miocene African sites will help to categorise the as yet understudied African community patterns of Hyaenidae.

Acknowledgements

We would like to thank Franziska “Poppy” Pezzei for her suggestion of applying for the Otterborg grant and Thorben Schöfisch for his help with the application. We would like to thank Chun Hei Ho for allowing us to borrow his camera equipment and for patient guidance in using his equipment. Thanks to Christiane Funk and Doreen Bayer of the Museum für Naturkunde, Katrin Krohmann and Irina Ruf of the Senckenberg Naturmuseum, Jan Decher and Christian Montermann of the Alexander Koenig Zoological Research Museum, Emmanuel Gilissen of the Royal Museum for Central Africa, Pepijn Kamminga of Naturalis Biodiversity Center, Paolo Agnelli of La Specola and Daniela Kalthoff of Naturhistoriska Riksmuseet for allowing us to visit their collections. Your guidance, help and answers to our questions were much appreciated.

References

- Anderson MJ. 2001. Non-Parametric MANOVA. *Austral Ecology*:32–46.
- Anderson MJ. 2006. Distance-Based Tests for Homogeneity of Multivariate Dispersions. *Biometrics* 62:245–253. DOI: 10.1111/J.1541-0420.2005.00440.X.
- Anderson MJ, Walsh DCI. 2013. PERMANOVA, ANOSIM, and the Mantel test in the face of heterogeneous dispersions: What null hypothesis are you testing? *Ecological Monographs* 83:557–574. DOI: 10.1890/12-2010.1.
- Anderson MJ, Walsh DCI, Robert Clarke K, Gorley RN, Guerra-Castro E. 2017. Some solutions to the multivariate Behrens–Fisher problem for dissimilarity-based analyses. *Australian and New Zealand Journal of Statistics* 59:57–79. DOI: 10.1111/anzs.12176.
- Andersson K. 2004. Elbow-joint morphology as a guide to forearm function and foraging behaviour in mammalian carnivores. *Zoological Journal of the Linnean Society* 142:91–104. DOI: 10.1111/j.1096-3642.2004.00129.x.
- Bekoff M. 1977. *Canis latrans*. *Mammalian Species*:1–9. DOI: 10.2307/3503817.
- Bingham J, Purchase G k. 2002. Reproduction in the jackals *Canis adustus* Sundevall, 1846, and *Canis mesomelas* Schreber, 1778 (Carnivora: Canidae), in Zimbabwe. *African Zoology* 37:21–26. DOI: 10.1080/15627020.2002.11657150.

- 568 Coca-Ortega C, Pérez-Claros JA. 2019. Characterizing ecomorphological patterns in hyenids: A
569 multivariate approach using postcanine dentition. *PeerJ* 2019:e6238. DOI:
570 10.7717/PEERJ.6238/SUPP-4.
- 571 Coelho L, Romero D, Queirolo D, Guerrero JC. 2018. Understanding factors affecting the
572 distribution of the maned wolf (*Chrysocyon brachyurus*) in South America: Spatial
573 dynamics and environmental drivers. *Mammalian Biology* 92:54–61. DOI:
574 10.1016/j.mambio.2018.04.006.
- 575 Dexter E, Rollwagen-Bollens G, Bollens SM. 2018. The trouble with stress: A flexible method
576 for the evaluation of nonmetric multidimensional scaling. *Limnology and Oceanography:*
577 *Methods* 16:434–443. DOI: 10.1002/LOM3.10257.
- 578 Dietz JM. 1985. *Chrysocyon brachyurus*. *Mammalian Species*:1–4. DOI: 10.2307/3503796.
- 579 Egeland AG, Egeland CP, Bunn HT. 2008. Taphonomic Analysis of a Modern Spotted Hyena
580 (*Crocuta crocuta*) Den from Nairobi, Kenya. *Journal of Taphonomy* 6:275–299.
- 581 Ewer RF. 1998. *The Carnivores*. New York: Cornell University Press.
- 582 Feibel CS. 2003. Stratigraphy and depositional history of the Lothagam sequence. In: Leakey M,
583 Harris J eds. *Lothagam: the dawn of humanity in eastern Africa*. New York: Columbia
584 University Press, 17–30. DOI: 10.7312/leak11870-002.
- 585 Fisher RonaldA. 1921. On the “Probable Error” of a Coefficient of Correlation Deduced from a
586 Small Sample. *Metron*:3–32.
- 587 Hastie T. 1989. Discussion. *Technometrics* 31:1–23.
- 588 Hastie T, Tibshirani R, Buja A. 1994. Flexible discriminant analysis by optimal scoring. *Journal*
589 *of the American Statistical Association* 89:1255–1270. DOI:
590 10.1080/01621459.1994.10476866.
- 591 Hastie T, Tibshirani R, Leisch F, Hornik K, Ripley BrianD. 2022. mda: Mixture and Flexible
592 Discriminant Analysis.

- Hayssen V, Noonan P. 2021. *Crocota crocota* (Carnivora: Hyaenidae). *Mammalian Species* 53:1–22. DOI: 10.1093/mspecies/seab002.
- Hildebrand M. 1954. Comparative morphology of the body skeleton of the recent Canidae. *Univ. Calif Publ Zool. Sci.* 52:399–470.
- Holm S. 1979. A Simple Sequentially Rejective Multiple Test Procedure. *Scandinavian Journal of Statistics* 6:65–70.
- Janis CM, Wilhelm PB. 1993. Were there mammalian pursuit predators in the tertiary? Dances with wolf avatars. *Journal of Mammalian Evolution* 1:103–125. DOI: 10.1007/BF01041590.
- Kassambara A. 2023. ggpubr: “ggplot2” Based Publication Ready Plots.
- Keesey TM. 2023. Silhouette Image Collection - PhyloPic. Available at <https://www.phylopic.org/collections/be14faff-9e89-4bf7-9e00-767cc6c666dd> (accessed August 11, 2023).
- Koehler CE, Richardson PRK. 1990. *Proteles cristatus*. *Mammalian Species*:1–6. DOI: 10.2307/3504197.
- Kruskal JB. 1964. Nonmetric multidimensional scaling: A numerical method. *Psychometrika* 29:115–129. DOI: 10.1007/BF02289694.
- Kuhn M. 2022. caret: Classification and Regression Training.
- Kurtén B. 1968. *Pleistocene mammals of Europe*. London: Weidenfeld & Nicolson.
- Leakey MG. 2003. Introduction. In: Leakey MG, Harris JM eds. *Lothagam: the dawn of humanity in eastern Africa*. The Dawn of Humanity in Eastern Africa. New York: Columbia University Press, 1–14.
- Leakey MG, Harris JM. 2003. Lothagam: Its significance and contributions. In: Leakey M, Harris J eds. *Lothagam: the dawn of humanity in eastern Africa*. New York: Columbia University Press, 625–660. DOI: 10.7312/leak11870-025.

- Legendre P, Legendre L. 1998. *Numerical Ecology*. Amsterdam: Elsevier Science B.V.
- Legendre P, Oksanen J, ter Braak CJF. 2011. Testing the significance of canonical axes in redundancy analysis. *Methods in Ecology and Evolution* 2:269–277. DOI: 10.1111/J.2041-210X.2010.00078.X.
- Mardia KV, Kent JT, Bibby JM. 1979. *Multivariate Analysis*. London: Academic Press.
- Martinez Arbizu P. 2020. pairwiseAdonis: Pairwise multilevel comparison using adonis.
- Martín-Serra A, Figueirido B, Palmqvist P. 2016. In the pursuit of the predatory behavior of Borophagines (Mammalia, Carnivora, Canidae): inferences from forelimb morphology. *Journal of Mammalian Evolution* 23:237–249. DOI: 10.1007/S10914-016-9321-5/TABLES/5.
- Matthews LH. 1939. The Bionomics of the spotted hyæna, *Crocota crocuta* Erxl. *Proceedings of the Zoological Society of London* 109A:43–56. DOI: 10.1111/j.1096-3642.1939.tb00046.x.
- McDougall I, Feibel CS. 2003. Numerical age control for the Miocene-Pliocene succession at Lothagam, a hominoid-bearing sequence in the Northern Kenya Rift. In: Leakey M, Harris J eds. *Lothagam: the dawn of humanity in eastern Africa*. New York: Columbia University Press, 43–64. DOI: 10.7312/LEAK11870-004/HTML.
- Mech LD. 1974. *Canis lupus*. *Mammalian Species*:1–6. DOI: 10.2307/3503924.
- Mills MGL. 1982. *Hyaena brunnea*. *Mammalian Species*:1. DOI: 10.2307/3504059.
- Nichols D. 2023. Coloring for Colorblindness. Available at <http://www.davidmathlogic.com/colorblind/> (accessed August 11, 2023).
- Nowak RM, Paradiso JL. 1983. *Walker’s Mammals of the World*. Baltimore: Johns Hopkins University Press. DOI: 10.2307/1381225.
- Oksanen J, Simpson GL, Blanchet FG, Kindt R, Legendre P, Minchin PR, O’Hara RB, Solymos P, Stevens MHH, Szoecs E, Wagner H, Barbour M, Bedward M, Bolker B, Borcard D,

Carvalho G, Chirico M, De Caceres M, Durand S, Evangelista HBA, FitzJohn R, Friendly M, Furneaux B, Hannigan G, Hill MO, Lahti L, McGlinn D, Ouellette M-H, Ribeiro Cunha E, Smith T, Stier A, Ter Braak CJF, Weedon J. 2022. vegan: Community Ecology Package.

Pennycuik CJ. 1975. On the running of the gnu (*Connochaetes Taurinus*) and other animals. *Journal of Experimental Biology* 63:775–799. DOI: 10.1242/jeb.63.3.775.

Posit team. 2023. RStudio: Integrated development environment for R.

R Core Team. 2022. R: A language and environment for statistical computing.

Rieger I. 1981. *Hyaena hyaena*. *Mammalian Species*:1–5. DOI: 10.2307/41353899.

Samuels JX, Meachen JA, Sakai SA. 2013. Postcranial morphology and the locomotor habits of living and extinct carnivorans. *Journal of Morphology* 274:121–146. DOI: 10.1002/jmor.20077.

Samuels JX, Van Valkenburgh B. 2008. Skeletal indicators of locomotor adaptations in living and extinct rodents. *Journal of Morphology* 269:1387–1411. DOI: 10.1002/jmor.10662.

Shapiro SS, Wilk MB. 1965. An analysis of variance test for normality (complete samples). *Biometrika* 52:591–611. DOI: 10.1093/biomet/52.3-4.591.

Sillero-Zubiri C, Hoffmann M, Macdonald DW. 2004. *Canids: Foxes, Wolves, Jackals and Dogs. Status survey and conservation action plan*. Gland and Cambridge.

Spoor CF, Badoux DM. 1988. Descriptive and functional myology of the back and hindlimb of the striped hyena (*Hyaena hyaena*, L. 1758). *Anatomischer Anzeiger* 167:313–321.

Strauss RE, Bookstein FL. 1982. The Truss: Body Form Reconstructions in Morphometrics. *Systematic Biology* 31:113–135. DOI: 10.1093/SYSBIO/31.2.113.

Turner A, Antón M, Werdelin L. 2008. Taxonomy and evolutionary patterns in the fossil Hyaenidae of Europe. *Geobios* 41:677–687. DOI: 10.1016/j.geobios.2008.01.001.

- 667 Van Valkenburgh B. 1987. Skeletal indicators of locomotor behavior in living and extinct
668 carnivores. *Journal of Vertebrate Paleontology* 7:162–182. DOI:
669 10.1080/02724634.1987.10011651.
- 670 Weihs C, Ligges U, Luebke K, Raabe N. 2005. klaR Analyzing German Business Cycles. In:
671 Baier D, Decker R, Schmidt-Thieme L eds. *Data Analysis and Decision Support*. Berlin:
672 Springer-Verlag, 335–343.
- 673 Werdelin L. 2003. Mio-Pliocene Carnivora from Lothagam, Kenya. In: Leakey MG, Harris JM
674 eds. *Lothagam: The Dawn of Humanity in Eastern Africa*. New York: Columbia
675 University Press, 261–328. DOI: 10.7312/leak11870-013.
- 676 Werdelin L, Solounias N. 1996. The evolutionary history of hyenas in Europe and western Asia
677 during the Miocene. *The evolution of western Eurasian Neogene mammal faunas*:290–
678 306.
- 679 Werdelin L, Turner A. 1996. Turnover in the guild of larger carnivores in Eurasia across the
680 Miocene-Pliocene boundary. *Acta Zoologica Cracoviensia* 39:585–592.
- 681 Wickham H. 2016. *ggplot2: Elegant Graphics for Data Analysis*. Springer-Verlag New York.
- 682 Wickham H, Averick M, Bryan J, Chang W, McGowan LD, François R, Grolemund G, Hayes A,
683 Henry L, Hester J, Kuhn M, Pedersen TL, Miller E, Bache SM, Müller K, Ooms J,
684 Robinson D, Seidel DP, Spinu V, Takahashi K, Vaughan D, Wilke C, Woo K, Yutani H.
685 2019. Welcome to the {tidyverse}. *Journal of Open Source Software* 4:1686. DOI:
686 10.21105/joss.01686.
- 687 Wikimedia commons. 2023b.File:Locator map of Kenya in Africa.svg. Available at
688 https://commons.wikimedia.org/wiki/File:Locator_map_of_Kenya_in_Africa.svg
689 (accessed September 24, 2023).
- 690 Wikimedia commons. 2023a.File:Kenya sat.png. Available at
691 https://commons.wikimedia.org/wiki/File:Kenya_sat.png (accessed September 24, 2023).

692 Wilke CO, Wiernik BM. 2022. ggtext: Improved Text Rendering Support for “ggplot2.”

693 Wynn JG. 2003. Miocene and Pliocene paleosols of Lothagam. In: Leakey M, Harris J eds.

694 *Lothagam: the dawn of humanity in eastern Africa*. New York: Columbia University

695 Press, 31–42. DOI: 10.7312/leak11870-003.

696

Figure 1

Map of Kenya showing the location of Lothagam, with the fossil site on the right.

Maps of Africa and Kenya were obtained from Wikimedia Commons (2023a; 2023b). The map of Lothagam was obtained from Google Earth Pro (Maxar Technologies and Airbus).

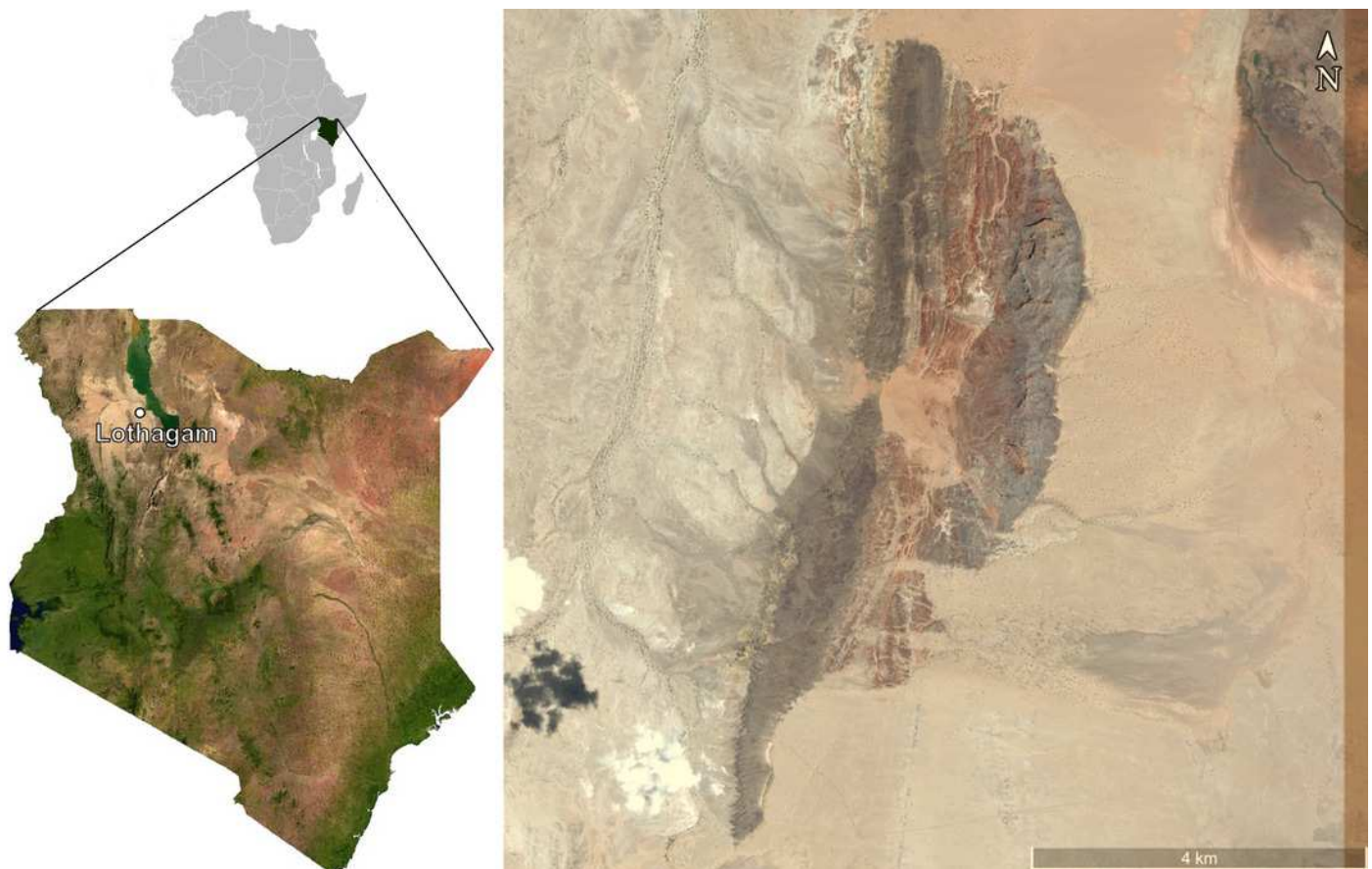


Figure 2

The left anterior humerus, left anterior radius, left lateral ulna, left anterior femur and dorsal right manus of specimen KNM-LT 23145 (*Ictitherium ebu*).

Scalebar is 10 cm.



Figure 3

Measurements of the postcrania used in the project, based on Samuels & Van Valkenburgh (2008) and Samuels, Meachen and Sakai (2013).

The specimen figured is NRM 20155145 (*Canis lupus*) and shows the left anterior humerus, left anterior radius, left lateral ulna, left anterior femur and dorsal right manus (not to scale).

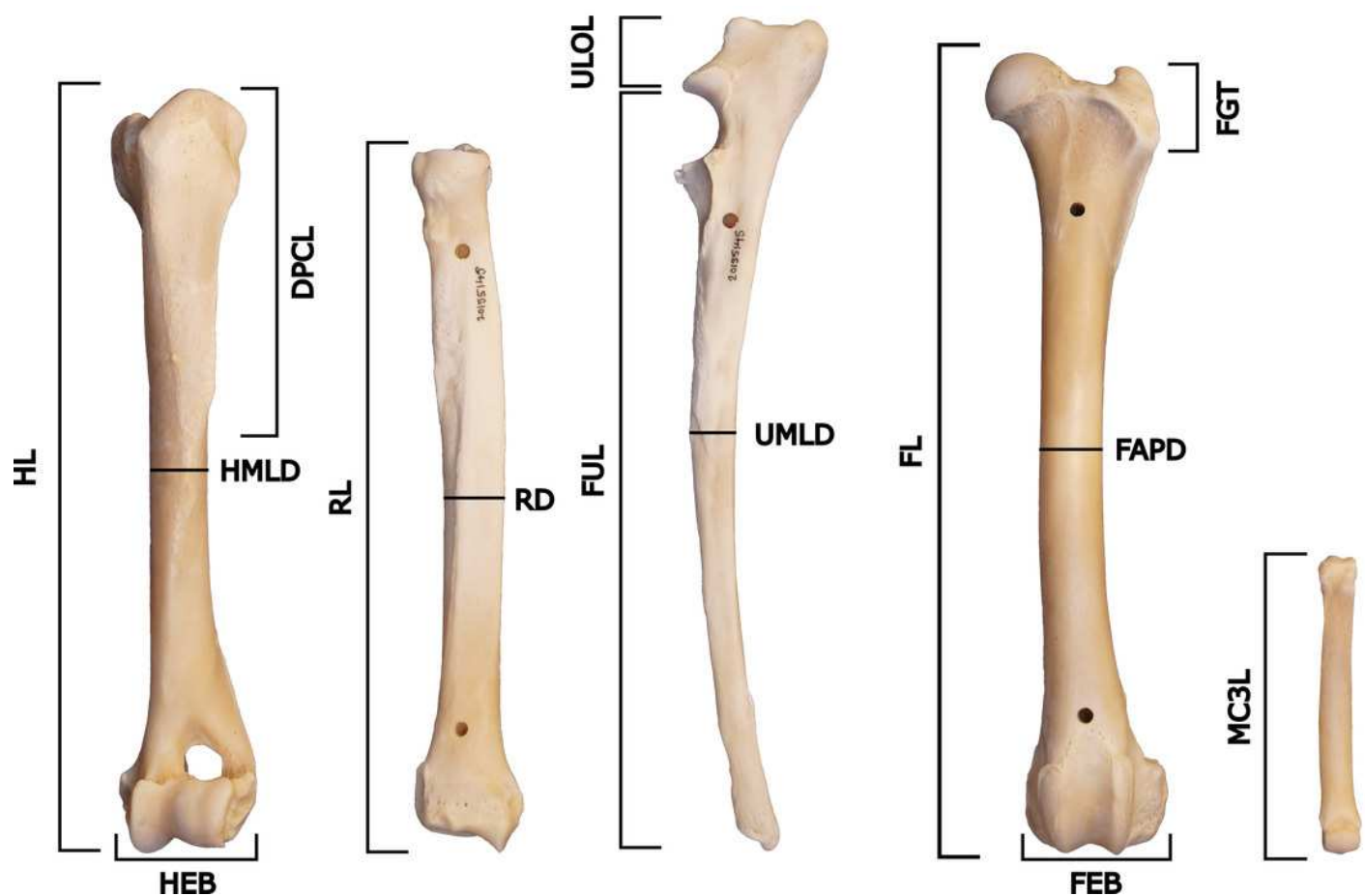


Figure 4

Schematic representation of the elbow joint with truss coordinates and distances marked out as dots and lines respectively. Figure adapted from Andersson (2004).

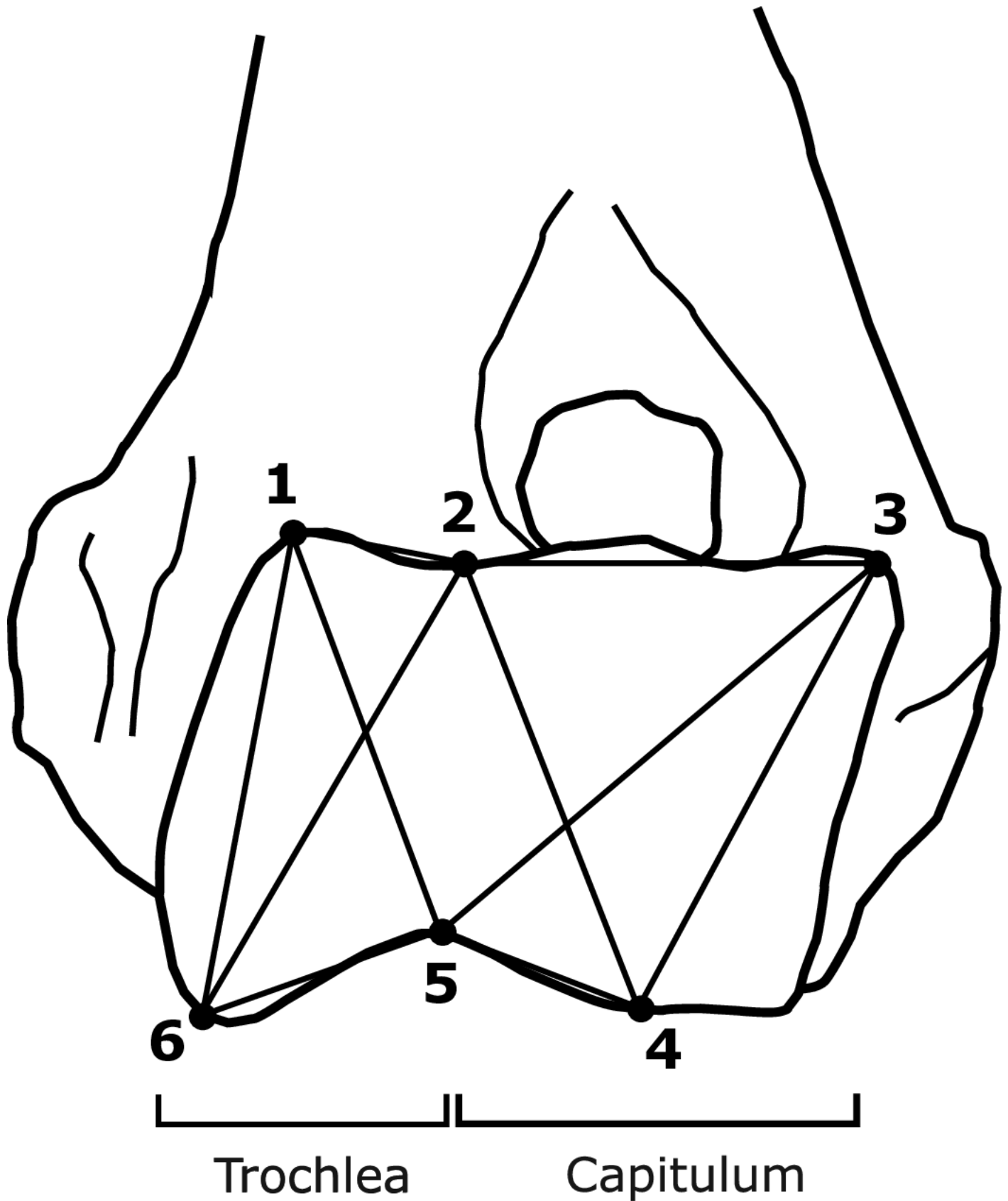


Figure 5

Boxplots of the species for the three most discriminant limb ratios.

(A). Branchial index. (B). Humeral epicondylar index. (C). Femoral epicondylar index. C = Coyote, W = Wolf, Mw = Maned wolf, Sp = Spotted Hyaena, St = Striped hyaena, le = *Ictitherium ebu*, Sj = Side-striped jackal, Bh = Brown hyaena, Aw = Aardwolf, F = Fox.

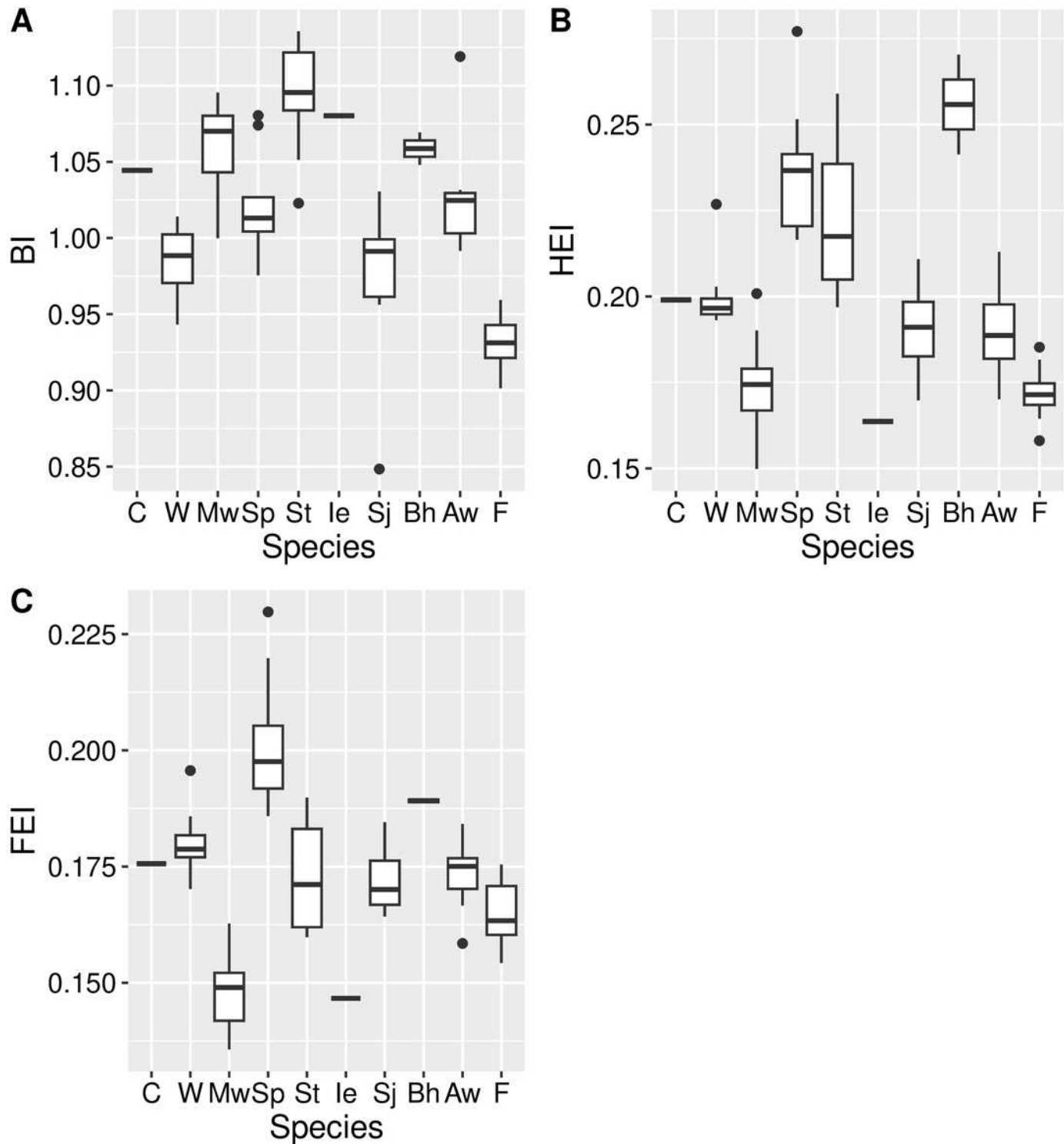


Figure 6

NMDS plot of the morphometric indices.

Species are labelled by shape, family by colour and size by largeness of the dots. Minimum convex polygons for each species are shown in the colour of their family. *I. ebu* is plotted as a black star. NMDS1 is inverted to plot smaller species on the left and larger species on the right. Species silhouettes except for *Ictitherium ebu* from Phylopic (Keesey 2023). Silhouette of *Ictitherium ebu* traced from the reconstruction by Javier Herbozo.

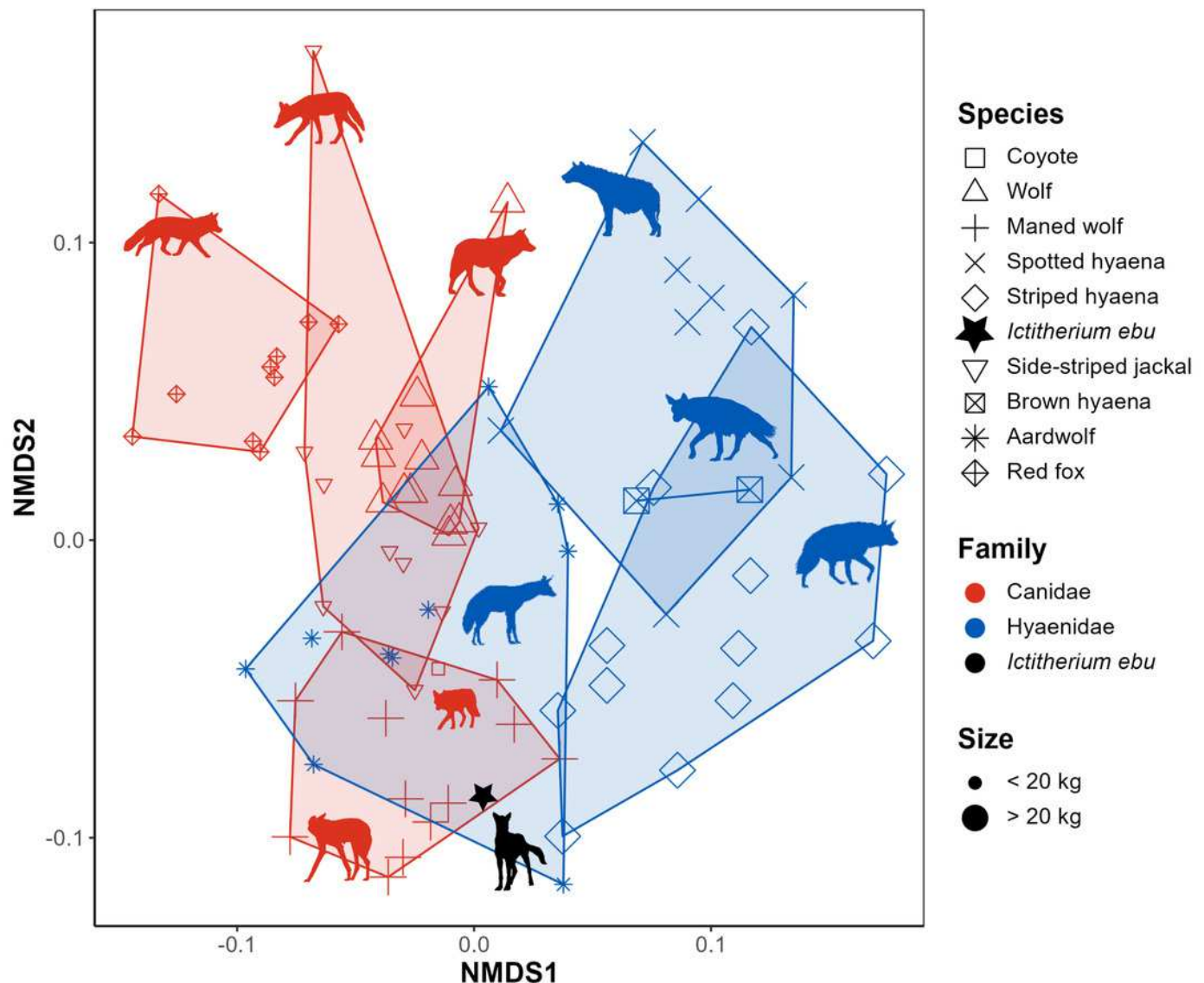


Figure 7

Flexible discriminant analysis of the morphometric indices.

Species are labelled by shape, family by colour and size by largeness of the dots. Minimum convex polygons for each species are shown in the colour of their family. The predicted value of *I. ebu* is plotted as a black star. CV1 is inverted to plot smaller species on the left and larger species on the right. Species silhouettes except for *Ictitherium ebu* from Phylopic (Keesey 2023). Silhouette of *Ictitherium ebu* traced from the reconstruction by Javier Herbozo.

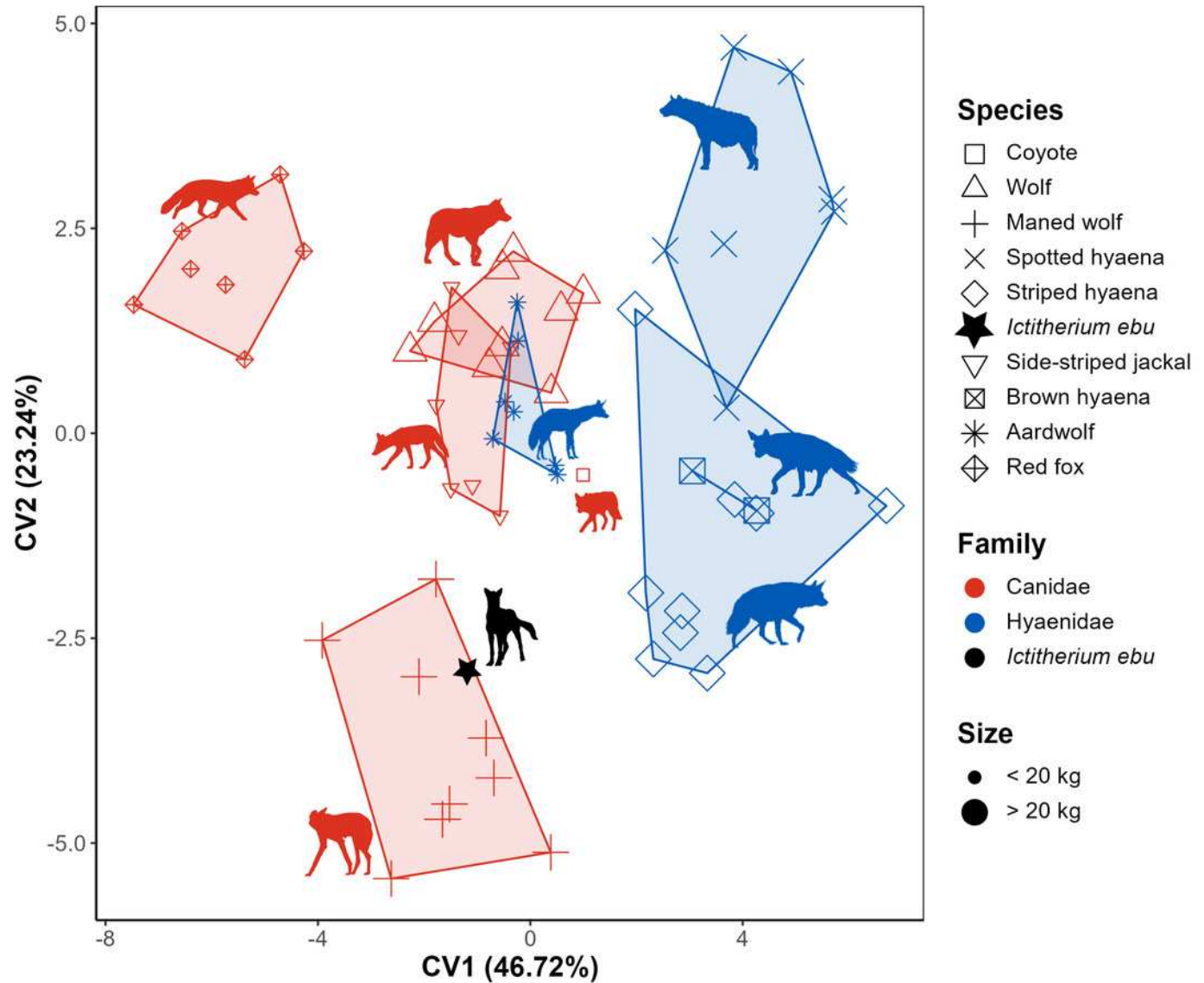


Figure 8

(A) Family, (B) locomotion and (C) habitat model strip charts.

Points are jittered to allow for a clearer view of the data. Groups are labelled by colour, species by shape. The prediction of *I. ebu* is plotted as a line. Silhouettes of *Ictitherium ebu* traced from the reconstruction by Javier Herbozo.

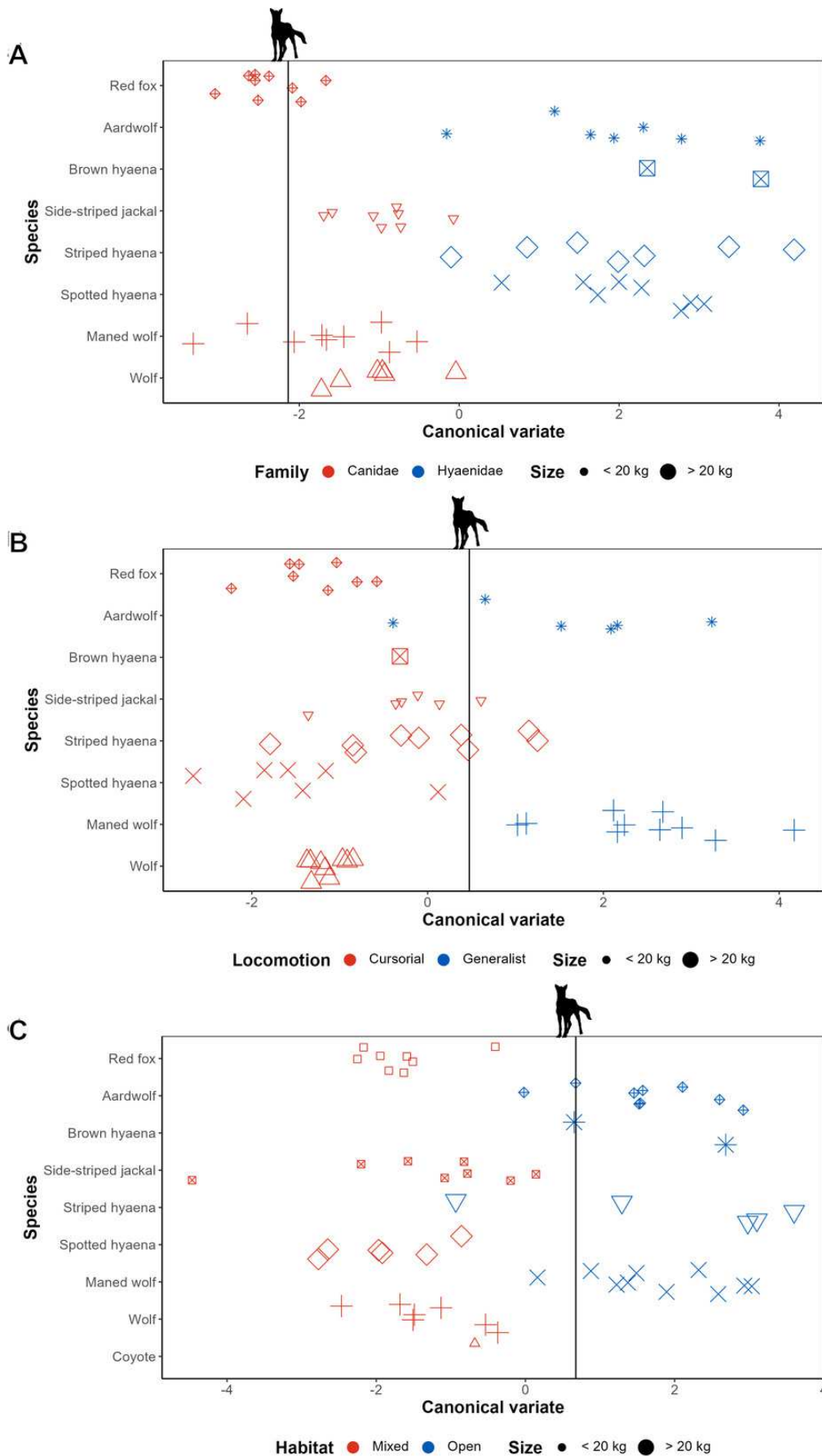


Figure 9

NMDS plot of the truss analysis.

Species are labelled by shape and family by colour. Minimum convex polygons for each species are shown in the colour of their family. The predicted value of *I. ebu* is plotted as a black star. NMDS2 is plotted in reverse to be able to more easily compare it to the linear NMDS. Species silhouettes except for *Ictitherium ebu* from Phylopic (Keesey 2023). Silhouette of *Ictitherium ebu* traced from the reconstruction by Javier Herbozo.

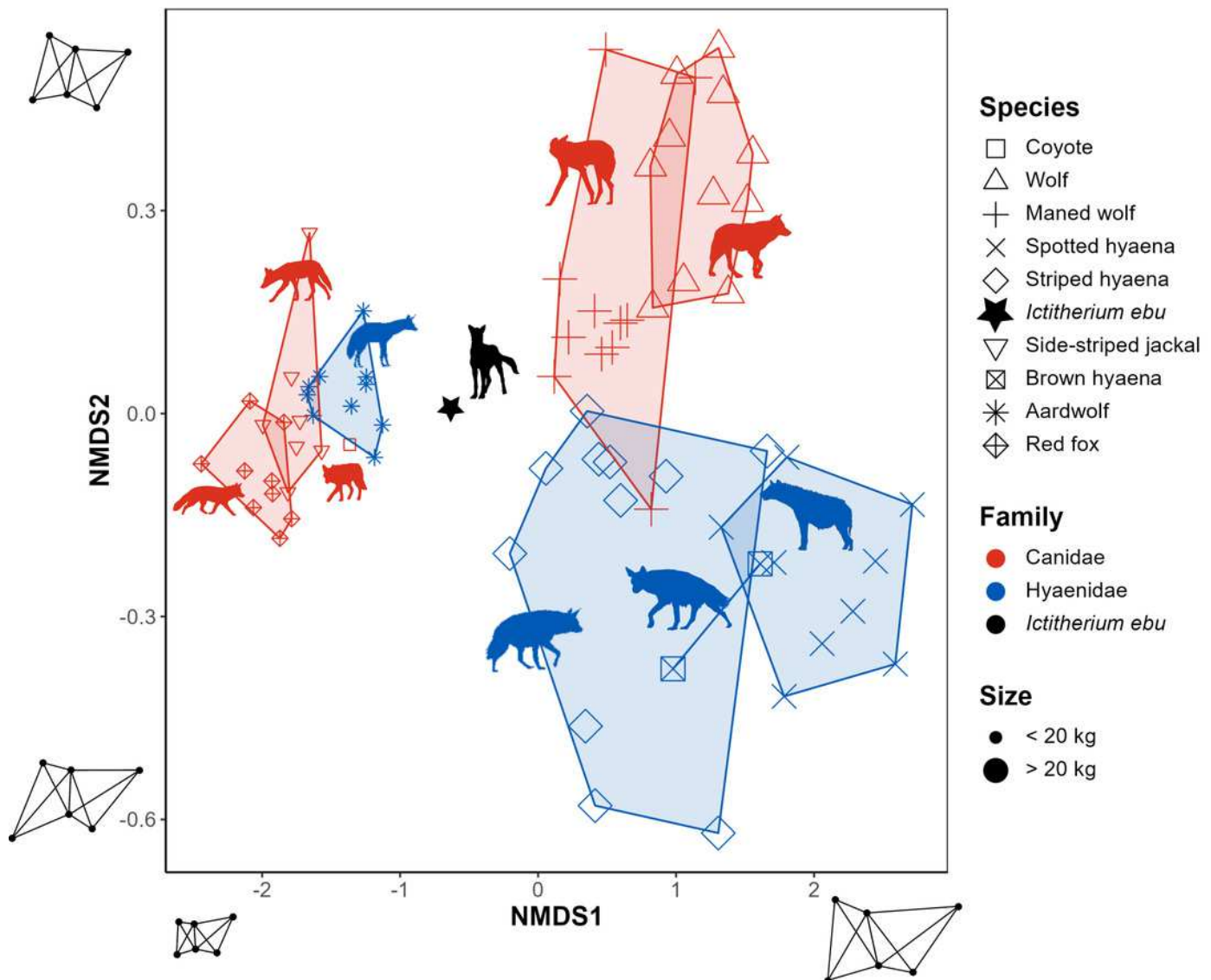


Figure 10

Flexible discriminant analysis of the truss distances.

Species are labelled by shape and family by colour. Minimum convex polygons for each species are shown in the colour of their family. The predicted value of *I. ebu* is plotted as a black dot. Axis 2 was plotted horizontally and axis 1 vertically, with axis 2 reversed for ease of comparison to the other plots. Species silhouettes except for *Ictitherium ebu* from Phylopic (Keesey 2023). Silhouette of *Ictitherium ebu* traced from the reconstruction by Javier Herbozo.

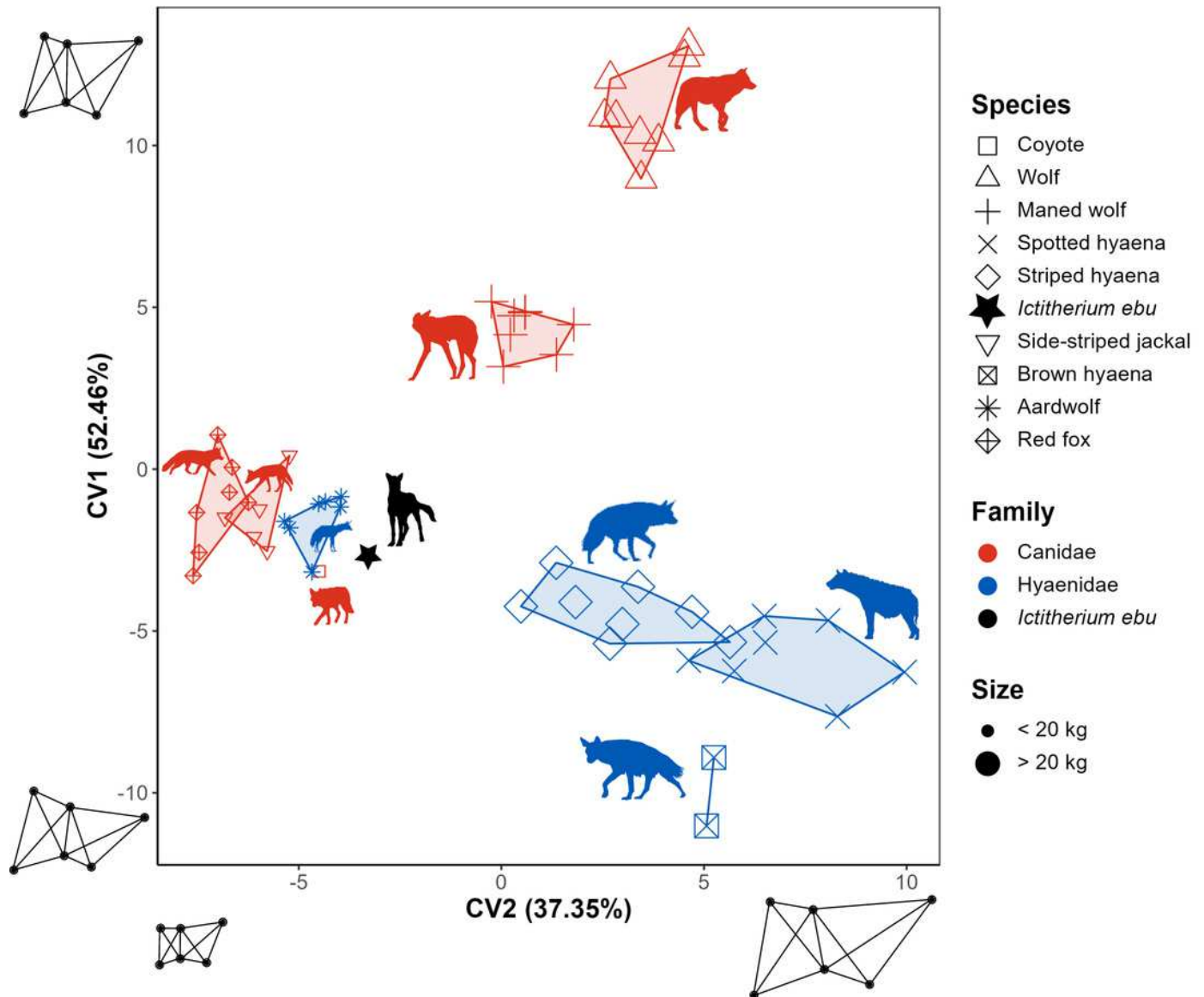


Figure 11

Family (A), locomotion (B) and habitat (C) model strip charts.

Points are jittered to allow for a clearer view of the data. Groups are labeled by colour, species by shape. The prediction of *I. ebu* is plotted as a line. Silhouettes of *Ictitherium ebu* traced from the reconstruction by Javier Herbozo.

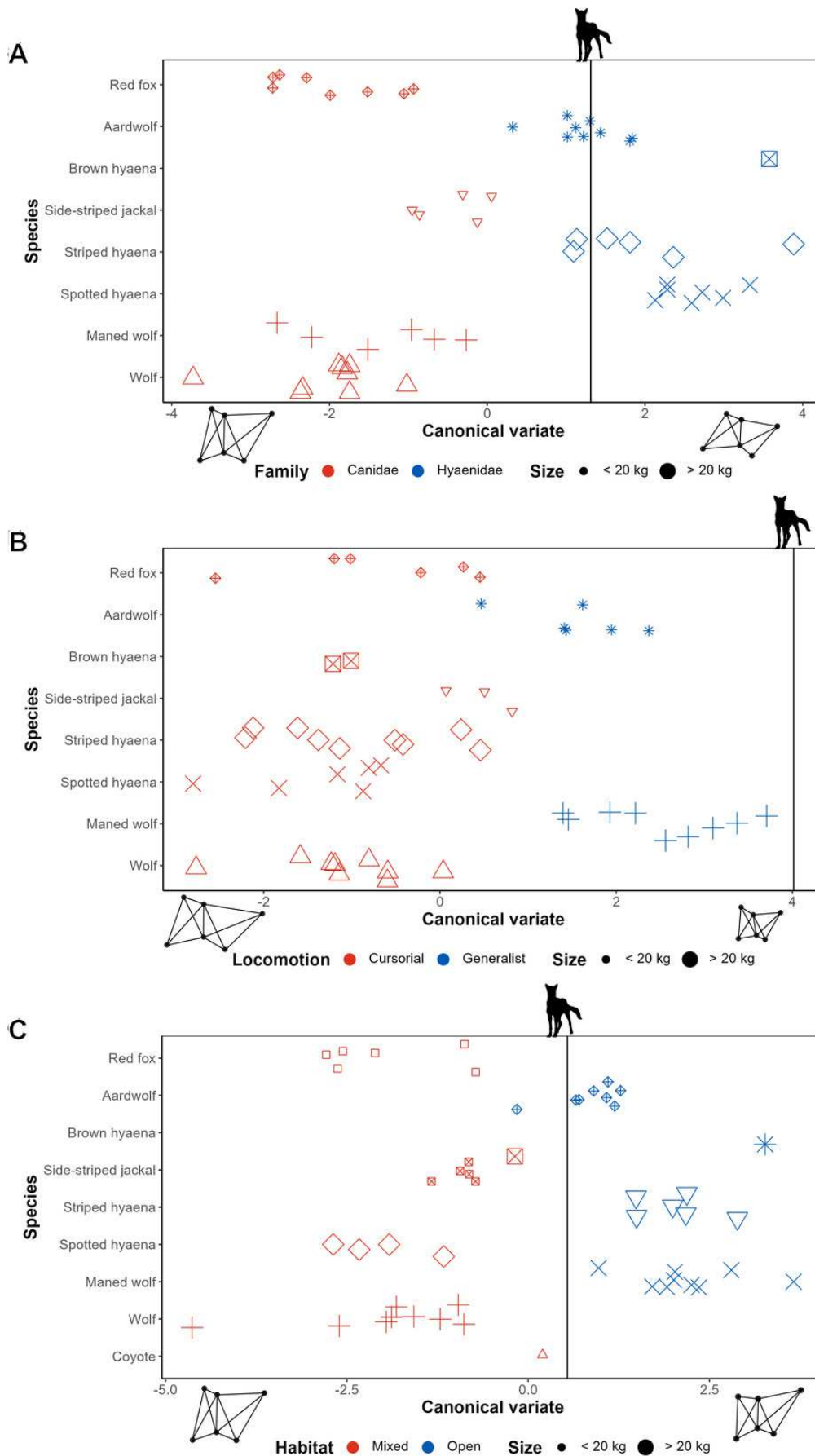


Table 1 (on next page)

The species used in this study including number of specimens, their locomotor type, habitat and body mass.

I. ebu* was hypothesised to be cursorial by Werdelin (2003). **The Lower Nawata where *I. ebu* was found represents a mixed habitat (Wynn 2003). * Body mass estimated by Werdelin (2003). 1. Koehler & Richardson (1990). 2. Spoor & Badoux (1988). 3. Rieger (1981). 4. Mills (1982). 5. Hayssen & Noonan (2021). 6. Matthews (1939). 7. Sillero-Zubiri *et al.* (2004). 8. Mech (1974). 9. Hildebrand (1954). 10. Janis & Wilhelm (1993). 11. Coelho *et al.* (2018). 12. Bekoff (1977). 13. Bingham & Purchase (2002). 14. Nowak & Paradiso (1983). 15. Dietz (1985).

1

Family	Genus	Species	Common name	Locomotor type	Habitat	Body mass (kg)	n
Hyaenidae	<i>Ictitherium</i> [†]	<i>ebu</i> [†]	n.a.	Cursorial*	Mixed**	10-15***	1
Hyaenidae	<i>Proteles</i>	<i>cristatus</i>	Aardwolf	Generalist ¹	Open ¹	47-79 ¹	10
Hyaenidae	<i>Hyaena</i>	<i>hyaena</i>	Striped hyaena	Cursorial ²	Open ³	22-55 ³	12
Hyaenidae	<i>Parahyaena</i>	<i>brunnea</i>	Brown hyaena	Cursorial ⁴	Open ⁴	28-47.5 ⁴	2
Hyaenidae	<i>Crocuta</i>	<i>crocuta</i>	Spotted hyaena	Cursorial ⁵	Mixed ⁶	47-79 ⁵	9
Canidae	<i>Lupulella</i>	<i>adusta</i>	Side-striped jackal	Cursorial ⁷	Mixed ⁷	8-10 ¹³	10
Canidae	<i>Vulpes</i>	<i>vulpes</i>	Red fox	Cursorial ⁷	Mixed ⁷	3-14 ¹⁴	10
Canidae	<i>Canis</i>	<i>lupus</i>	Wolf	Cursorial ⁸	Mixed ⁸	18-80 ⁸	12
Canidae	<i>Chrysocyon</i>	<i>brachyurus</i>	Maned wolf	Generalist ^{9,10}	Open ¹¹	23 ¹⁵	12
Canidae	<i>Canis</i>	<i>latrans</i>	Coyote	Cursorial ¹²	Mixed ¹²	7-20 ¹²	1

2

Table 2(on next page)

Measurements according to Samuels & Van Valkenburgh (2008) and Samuels, Meachen and Sakai (2013), with RD added.

1
2

Measurement	Description
HL	Greatest length of the humerus
HMLD	Midshaft mediolateral diameter of the humerus
DPCL	Length of the deltopectoral crest
HEB	Epicondylar breadth of the distal humerus
RL	Greatest length of the radius
RD	Midshaft mediolateral diameter of the radius
FUL	Functional length of the ulna
UMLD	Midshaft mediolateral diameter of the ulna
ULOL	Length of the olecranon process of the ulna
MC3L	Greatest length of metacarpal 3
FL	Greatest length of the femur
FAPD	Midshaft anteroposterior diameter of the femur
FGT	Height of the greater trochanter of the femur
FEB	Epicondylar breadth of the distal femur

Table 3(on next page)

Indices following Samuels & Van Valkenburgh (2008) and Samuels, Meachen and Sakai (2013), with RRI, MCRI, MCHUM and HFI added and MANUS removed.

1

Index	Description
Shoulder moment index (SMI)	Deltopectoral crest length divided by functional length of the humerus (DPCL/HL). Indicates mechanical advantage of the deltoid and pectoral muscles acting across the shoulder joint.
Brachial index (BI)	Functional length of the radius divided by functional length of the humerus (RL/HL). Indicates relative proportions of proximal and distal elements of the forelimb.
Humeral robustness index (HRI)	Mediolateral diameter of humerus divided by functional length of the humerus (HMLD/HL). Indicates robustness of the humerus and its ability to resist bending and shearing stresses.
Humeral epicondylar index (HEI)	Epicondylar breadth of humerus divided by functional length of the humerus (HEB/HL). Indicates relative area available for the origins of the forearm flexors, pronators, and supinators.
Olecranon length index (OLI)	Olecranon process length divided by functional length of the ulna (ULOL/FUL). Indicates relative mechanical advantage of the triceps brachii and dorsoepitrochlearis muscles used in elbow extension. This is identical to the index of fossorial ability used by Hildebrand (1985).
Ulnar robustness index (URI)	Mediolateral diameter of ulna divided by functional length of the ulna (UMLD/FUL). Indicates robustness of the ulna and its ability to resist bending and shearing stresses, and relative area available for the origin and insertion of forearm and manus flexors, pronators, and supinators.
Femoral robustness index (FRI)	Anteroposterior diameter of femur divided by functional length of the femur (FAPD/FL). Indicates robustness of the femur and its ability to resist bending and shearing stresses (AP diameter is used due to transverse expansion of the femora in semiaquatic rodents).
Gluteal index (GI)	Length of distal extension of the greater trochanter of the femur divided by functional length of the femur (FGT/FL). Indicates relative mechanical advantage of the gluteal muscles used in retraction of the femur.
Femoral epicondylar index (FEI)	Epicondylar breadth of femur divided by the functional

length of the femur (FEB/FL). Indicates relative area available for the origins of the gastrocnemius and soleus muscles used in extension of the knee and plantar-flexion of the pes.

Radial robustness index (RRI)

Greatest length of the radius divided by the midshaft mediolateral diameter of the radius (RD/RL). Indicates robustness of the radius and its ability to resist bending and shearing stresses.

Metacarpal radial index (MCRI)

Greatest length of metacarpal 3 divided by the functional length of the radius (MC3L/RL). Indicates relative proportions of the third metacarpal compared to the radius.

Metacarpal humeral index
(MCHUM)

Greatest length of metacarpal 3 divided by the functional length of the humerus (MC3L/HL). Indicates relative proportions of the third metacarpal compared to the length of the humerus.

Humeral femoral index (HFI)

Functional length of the radius divided by the functional length of the femur(HL/FL). Indicates relative proportions of the humerus compared to the femur.

Table 4(on next page)

Results of the two-way permutational analysis of variance (PERMANOVA) of indices compared to species and family.

Df = Degrees of freedom. SumofSqs = Sum of Squares. R2 = R-squared F = F-statistic.

Pr(>F) = Significance.

1

	Df	SumOfSqs	R2	F	Pr(>F)
Family	2	0.23	0.24	24.08	0.001
Family:Species	7	0.40	0.42	12.07	0.001
Residual	69	0.33	0.34		
Total	78	0.95	1		

2

Table 5(on next page)

NMDS1 and NMDS2 loadings of the non-metric multidimensional scaling of the morphometric indices.

1

	NMDS1	NMDS2
SMI	-0.16	0.08
BI	-0.01	-0.06
HRI	-0.05	0.03
OLI	0.03	0.17
URI	-0.02	0.17
FRI	-0.03	0.04
GI	-0.03	0.05
FEI	-0.02	0.06
HEI	-0.12	0.04
RRI	0.01	0.12
MCRI	0.06	-0.0004
HFI	0.08	-0.01
MCHUM	-0.01	-0.05

2

Table 6(on next page)

NMDS1 and NMDS2 loadings of the non-metric multidimensional scaling for the truss analysis.

1

2	NMDS1	NMDS2
2-6	0.10	0.01
2-5	-1.53	-0.45
3-5	-0.03	-0.02
1-5	-0.02	-0.18
2-4	0.36	-0.18
5-6	3.43	0.71
4-5	3.12	0.07
3-4	-1.04	-0.11
2-3	2.15	0.37
1-2	-0.65	-0.02
1-6	0.44	-0.06